DOI: 10.21062/mft.2026.007 http://www.journalmt.com

Effect of Accelerated Aging on the Mechanical Properties of FFF-Manufactured Polymers

Marcel Kohutiar (0000-0002-4710-5913)[1], Martin Bednařík (0000-0002-7900-4762)[2], Ivan Labaj (0000-0002-8835-5548)[3], Róbert Janík (0000-0002-4178-1865)[3], Jan Hanzlík (0009-0001-5863-1062)[2], Michal Krbata (0000-0002-0520-8180)[1], Jakub Zatloukal[2]
[1]Faculty of Special Technology, Alexander Dubcek University of Trenčín, Ku Kyselke 469, 911 06 Trenčín, Slovakia. E-mail: marcel.kohutiar@tnuni.sk, michal.krbata@tnuni.sk
[2]Faculty of Technology, Department of Production Engineering, Tomas Bata University in Zlín, Vavrečkova 5669 760 01 Zlín, Czech Republic. E-mail: mbednarik@utb.cz, j_zatloukal@utb.cz, j_hanzlik@utb.cz
[3]Faculty of Industrial Technologies in Puchov, Alexander Dubcek University of Trenčín, Ivana Krasku 491/30 020 01 Púchov, Slovakia. E-mail: ivan.labaj@tnuni.sk, robert.janik@tnuni.sk

This study examines the effect of accelerated weathering on the mechanical and viscoelastic properties of thermoplastics produced by fused filament fabrication (FFF). Three polymers, acrylonitrile styrene acrylate (ASA), polyethylene terephthalate glycol (PETG), and polylactic acid (PLA), were subjected to alternating UV radiation and condensation cycles in a QUV chamber simulating environmental exposure. Tensile testing and dynamic mechanical analysis (DMA) were used to evaluate the changes in strength, stiffness, and glass-transition behavior. The results revealed distinct responses depending on the polymer structure. ASA maintained its ductility and even showed improved strength, confirming high UV resistance. PETG exhibited a moderate decrease in strength with negligible change in elongation, indicating partial photo-oxidation but stable viscoelastic behavior. PLA demonstrated the most significant stiffening and a noticeable upward shift of the glass-transition temperature due to crystallization and physical aging. Overall, short-term QUV exposure acted as a conditioning process, enhancing the thermal and structural stability of the tested FFF-printed polymers.

Keywords: Fused filament fabrication, Accelerated weathering, Dynamic mechanical analysis, Tensile strength, Thermoplastics

1 Introduction

Additive manufacturing (AM) has become an essential technology for the production of polymer components with complex geometries, reduced material waste, and rapid prototyping capabilities. Among the various AM methods, fused filament fabrication (FFF) is one of the most widely used techniques due to its low cost, design flexibility, and availability of thermoplastic filaments [1,2,3]. However, parts produced by FFF often exhibit anisotropic mechanical behavior and limited resistance to environmental degradation compared to conventionally manufactured polymers [4].

Polymeric materials used in outdoor or high-humidity environments are exposed to multiple degradation factors such as ultraviolet (UV) radiation, temperature fluctuations, and moisture condensation, which can lead to chain scission, oxidation, embrittlement, and loss of mechanical integrity [5]. The extent of these effects strongly depends on the chemical composition and morphology of the polymer, whether it is amorphous, semi-crystalline, or contains stabilizing copolymer segments [6]. Therefore, understanding how environmental factors influence the mechanical and viscoelastic performance of FFF-printed materials is crucial for ensuring their long-term reliability in engineering applications.

Previous studies have shown that UV exposure can cause either degradation or structural reinforcement in thermoplastics, depending on the exposure time and material type. Acrylonitrile styrene acrylate (ASA) is known for its high weather resistance and dimensional stability [7], polyethylene terephthalate glycol (PETG) combines good ductility with transparency but is moderately sensitive to UV radiation [8], and polylactic acid (PLA), though biodegradable and widely used, exhibits changes in crystallinity and stiffness under thermal and UV stress [9]. Nevertheless, only limited studies have systematically compared these three materials under identical QUV aging conditions using both tensile testing and dynamic mechanical analysis (DMA) to assess the evolution of mechanical and viscoelastic properties.

The main objective of this study is to provide a comprehensive evaluation of how accelerated weathering (UV and humidity cycles) affects the mechanical strength, stiffness, and glass-transition

behavior of ASA, PETG, and PLA polymers manufactured by FFF. The study aims to identify correlations between structural morphology and degradation mechanisms, contributing to a deeper understanding of the environmental durability and long-term stability of additively manufactured polymer components.

2 Materials and methods

The research was focused on evaluating the influence of accelerated weathering on the mechanical and dynamic-mechanical properties of polymeric materials manufactured by fused filament fabrication (FFF). Three types of thermoplastics commonly used in additive manufacturing were selected for the experiments – polylactic acid (PLA), polyethylene terephthalate glycol-modified (PETG), and acrylonitrile styrene acrylate (ASA).

Samples were produced using a Prusa i3 MK3S 3D printer via the FFF process from original Prusament filaments (PLA, PETG, ASA) with a diameter of 1.75 mm. Printing was carried out using a 0.4 mm nozzle and a 0.2 mm layer height. All samples were fabricated with uniform infill densities of 70%, 80%, 90%, and 100%, in the shape of standard tensile bars according to ISO 527-2 Type 1B [10]. For dynamic mechanical analysis (DMA), separate samples with dimensions 65 × 12.8 × 3.2 mm were prepared to match the Dual Cantilever geometry (Fig. 1) [10]. All DMA tests were performed on samples with 100 % infill to eliminate the influence of porosity and ensure a representative interpretation of the material's viscoelastic behavior. After printing, all samples were conditioned for 8 hours at room temperature (23 ± 2 °C) and subsequently stored in opaque containers to prevent spontaneous photodegradation prior to testing.

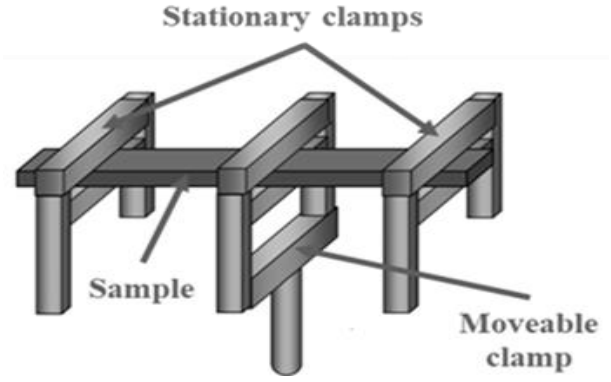

Fig. 1 *Dual Cantiliver geometry used in DMA analysis [12]*

The simulation of environmental degradation effects was performed using a QUV weathering tester (Q-LAB), which enables accelerated aging of polymers through alternating exposure to UV radiation and humidity according to ISO 4892-3 [11]. The testing cycle consisted of 8 hours of UV exposure (UVA-351 lamps) at 60 °C, followed by a 4-hour condensation cycle at 50 °C. Samples were subjected to seven complete cycles (total exposure time 84 hours), corresponding to a short-term outdoor exposure equivalent under Central European climatic conditions. After exposure, the samples were visually inspected and prepared for subsequent mechanical testing.

Static tensile tests were performed using a Shimadzu AG-X Plus universal testing machine at room temperature with a crosshead speed of 10 mm·min^{-1}. For each infill level and material type, ten samples were tested, and the average values of tensile strength (Rm) and elongation at break were calculated. The obtained data were processed using the Trapezium software integrated into the testing device. This method represents an important approach for understanding the mechanical behavior of polymers and identifying the mechanisms of their failure.

Fracture surface analysis after the tensile test was carried out using a confocal microscope Olympus OLS5100, and the acquired images were processed in OLS5100 software v3.1.

The dynamic mechanical analysis (DMA) was performed on a TA Instruments Q800 analyzer. The samples were mounted in the Dual Cantilever geometry (Fig. 1), and the measurements were conducted in the temperature range of 30–140 °C for ASA and 30–115 °C for PETG and PLA. These temperature ranges were selected to cover the glass-transition region (T_g) of each polymer; therefore, the upper temperature limits were adjusted accordingly. The heating rate was 3 °C·min^{-1}, with an amplitude of 15 μm, a frequency of 10 Hz, and a constant force of 1 N.

Measurements were performed for all three polymers (PLA, PETG, ASA) in both reference (non-aged) and UV-aged (degraded) states. For each material, three samples were analyzed, which was sufficient considering the nature of the measurements. The objective was to determine changes in the storage modulus (E'), loss modulus (E''), and loss factor ($tan\ \delta$), including the glass-transition temperature (T_g). The recorded data were evaluated using TA Universal Analysis 4.5A software. For each material, the dependencies of E', E'', and $tan\ \delta$ on temperature were processed according to the ASTM D4065 standard [13].

3 Results and discussion

As shown in Fig. 2, the ASA material exhibited a significant increase in tensile strength after accelerated weathering in the QUV chamber, while the elongation

at break remained almost unchanged. The tensile strength (Figure 2a) increased consistently with higher infill density for both the reference and QUV-aged samples. However, the QUV-exposed samples showed noticeably higher values across all infill levels, indicating that UV radiation and condensation cycles induced slight structural stiffening. The most pronounced improvement was observed for 100 % infill, where the tensile strength increased from 40.71 MPa (ASA Reference) to 55.58 MPa, representing an enhancement of approximately 36 %. Similar trends were observed for lower infill ratios, with increases ranging between 29–34%.

In contrast, the elongation at break (Fig. 2b) showed only marginal changes after UV exposure. The values of elongation fluctuated in a narrow range between 3.3% and 3.5%, suggesting that the elongation of ASA was largely preserved. This indicates that, despite the increase in stiffness and strength, the material did not become significantly more brittle. The results confirm the high environmental stability of ASA and its resistance to degradation processes induced by UV radiation and humidity [4,14].

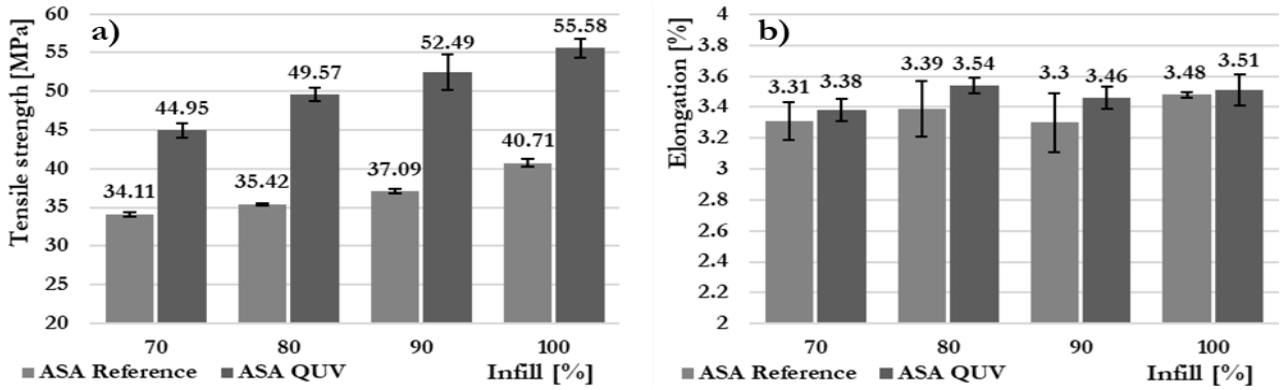

Fig. 2 *Comparison of mechanical properties of ASA before and after accelerated weathering: (a) Tensile strength as a function of infill density for reference and QUV-aged samples; (b) Elongation at break as a function of infill density for reference and QUV-aged samples*

As illustrated in Fig. 3, the PETG samples demonstrated a different response to accelerated weathering compared to ASA. The tensile strength (Fig. 3a) generally increased with higher infill density for both the reference and QUV-aged samples; however, a noticeable decrease in tensile strength occurred after UV and humidity exposure. For 100% infill, the tensile strength decreased from 80.87 MPa (PETG Reference) to 70.83 MPa, corresponding to a reduction of approximately 12%. Similar decreases were observed for lower infill ratios, ranging between 3% and 10%. This reduction in mechanical performance can be attributed to photo-oxidative degradation of the polymer backbone, leading to partial chain scission and reduced intermolecular cohesion between printed layers.

In contrast, the elongation at break (Fig. 3b) showed no significant variation after QUV exposure. The values of elongation remained within the range of 4.5–5.3%, indicating that PETG retained its ductile behavior and plastic deformation capability even after accelerated aging. The relatively stable elongation, despite the reduced strength, suggests that degradation affected mainly the load-bearing capacity rather than the overall deformability of the material [4,15].

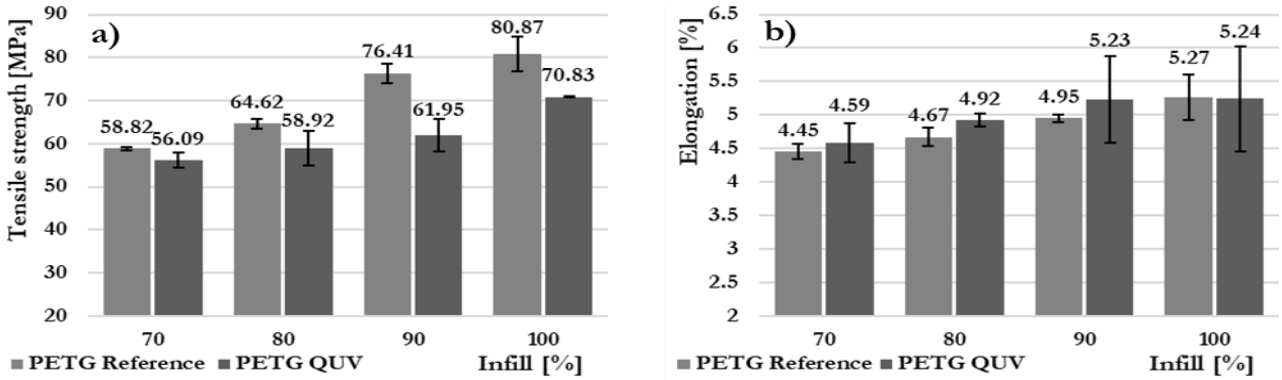

Fig. 4 *Comparison of mechanical properties of PETG before and after accelerated weathering: (a) Tensile strength as a function of infill density for reference and QUV-aged samples; (b) Elongation at break as a function of infill density for reference and QUV-aged samples*

As shown in Fig. 4, the PLA samples exhibited a clear increase in tensile strength after accelerated weathering, accompanied by a moderate improvement in elongation at break. The tensile strength (Fig. 4a) increased systematically with higher infill density for both reference and QUV-aged samples, while the post-exposure samples consistently reached higher values. For 100% infill, the tensile strength increased from 47.56 MPa (PLA Reference) to 71.87 MPa, representing an enhancement of approximately 51%. Similar upward trends were recorded for the lower infill levels, with increments ranging from 20% to 40%. This notable improvement can be attributed to structural rearrangement and secondary crystallization of PLA chains induced by thermal cycling and UV radiation during the QUV test. The increased crystallinity likely enhanced molecular packing and stiffness, resulting in higher tensile strength values [16,17].

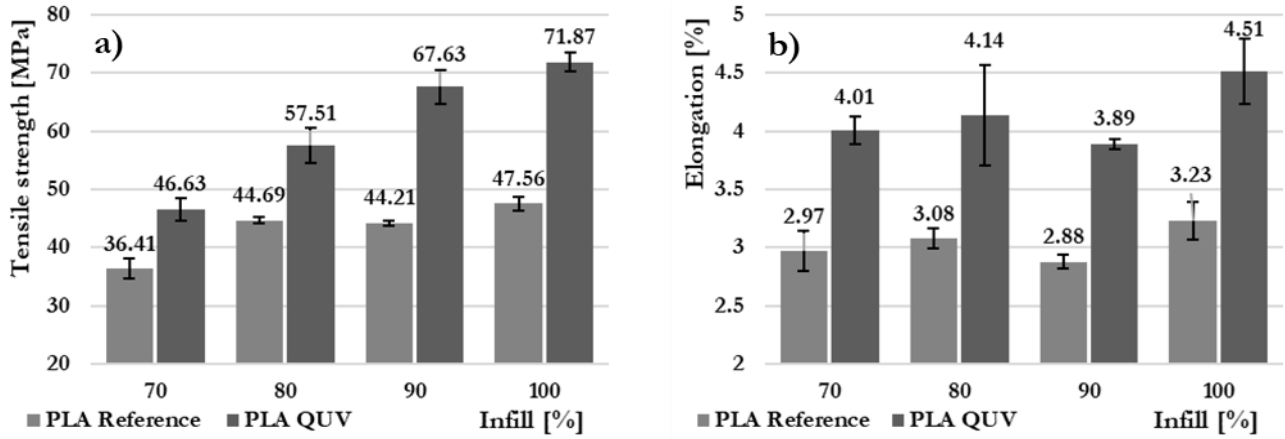

Fig. 4 *Comparison of mechanical properties of PLA before and after accelerated weathering: (a) Tensile strength as a function of infill density for reference and QUV-aged samples; (b) Elongation at break as a function of infill density for reference and QUV-aged samples*

The elongation at break (Fig. 4b) also showed a moderate increase after QUV exposure, with elongation values rising from approximately 3.0% for the reference samples to around 4.5% for the aged samples. This indicates that, in addition to improved stiffness, PLA retained or slightly improved its ability to deform plastically before fracture. The combined increase in both strength and elongation suggests that the accelerated weathering did not cause degradation but rather facilitated physical aging and partial ordering of the polymer matrix.

Overall, PLA showed a positive response to the accelerated weathering conditions used in this study. The results confirm that short-term UV and humidity exposure can promote mild structural reorganization, leading to increased mechanical stability and enhanced performance of PLA parts produced by FFF.

Fig. 5 shows the fracture surfaces of ASA samples after tensile testing, captured using a confocal microscope. The reference sample (Fig. 5a) exhibits a relatively rough and uneven fracture surface with distinct layer interfaces, indicating a ductile–brittle mixed failure mode typical for FFF-printed thermoplastics. The presence of irregular voids and tearing between deposited rasters suggests partial interlayer separation during tensile loading.

In contrast, the QUV-aged sample (Fig. 5b) reveals a smoother and more compact fracture surface, characterized by better fusion between adjacent filaments and less evidence of interlayer debonding. This change in surface morphology corresponds with the increased tensile strength measured after accelerated weathering, implying that short-term UV and humidity exposure enhanced local molecular rearrangement and possibly improved interlayer adhesion. The more continuous fracture profile and reduced microvoid content confirm that ASA maintained structural integrity and even experienced mild stiffening after environmental exposure [18].

As shown in Fig. 6, the fracture morphology of PETG samples after tensile testing reveals distinct differences between the reference and QUV-aged samples. The reference sample (Fig. 6a) exhibits a relatively smooth and continuous fracture surface with elongated filament structures and visible plastic deformation, confirming the ductile nature of PETG. Local tearing and filament stretching indicate gradual material failure and good interlayer adhesion typical for FFF-printed PETG.

In contrast, the QUV-aged sample (Fig. 6b) presents a rougher and more irregular fracture profile with pronounced voids and separated filament edges. These features suggest partial loss of interlayer cohesion and a transition toward a more brittle failure mode after exposure to UV radiation and humidity. The fragmented filament ends and fibrillar morphology correspond with the measured decrease in tensile strength, confirming that photo-oxidative

degradation and chain scission negatively affected the structural integrity of PETG [15,19]

As shown in Fig. 7, the fracture surfaces of PLA samples after tensile testing reveal pronounced morphological differences between the reference and QUV-aged samples. The reference sample (Fig. 7a) displays a highly fibrous fracture structure with numerous stretched and pulled filaments, indicating a ductile fracture mechanism associated with localized necking and interlayer tearing. The extensive filament deformation suggests good interlayer adhesion and significant plastic flow before rupture, typical for non-aged PLA. After exposure to UV radiation and condensation cycles, the QUV-aged sample (Fig. 7b) exhibits a smoother and more compact fracture surface with limited filament stretching and a narrower fracture zone. This morphological transition indicates reduced elongation and an increase in stiffness caused by secondary crystallization and partial chain reorganization during accelerated aging. The change in fracture appearance corresponds with the increase in tensile strength and the moderate rise in elongation observed in mechanical testing, confirming that the short-term UV exposure promoted structural ordering rather than degradation of the PLA matrix [16, 17].

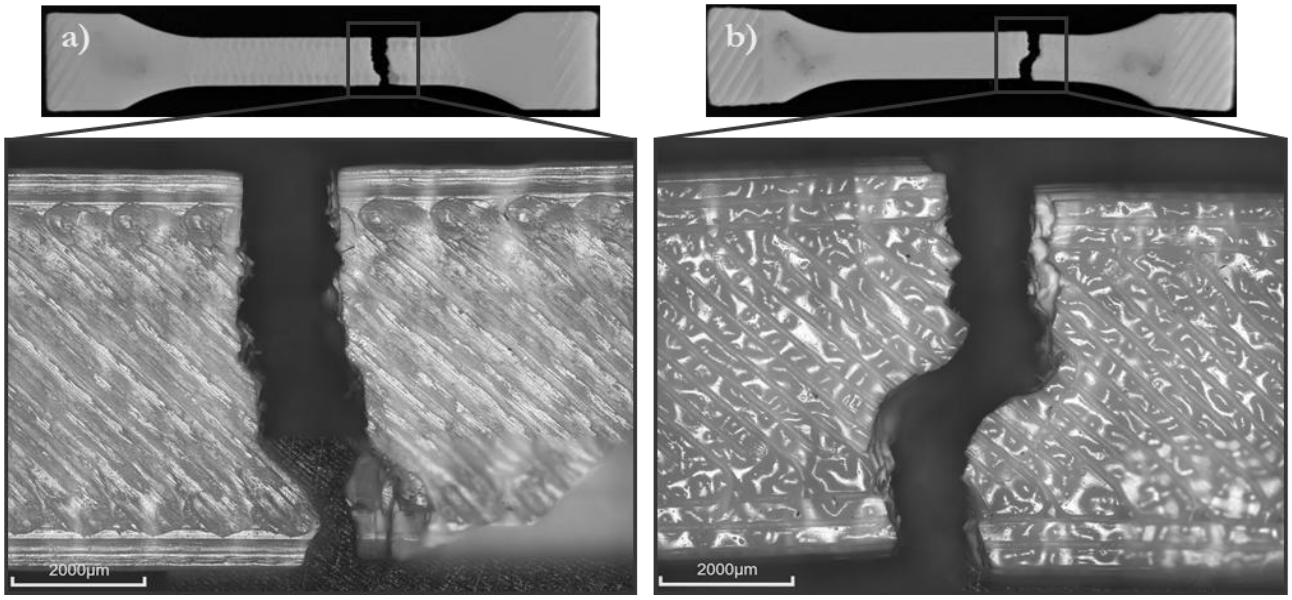

Fig. 5 *Fracture surfaces of ASA samples (100 % infill) after tensile testing observed by confocal microscopy: (a) reference sample (ASA Reference); (b) QUV-aged sample (ASA QUV)*

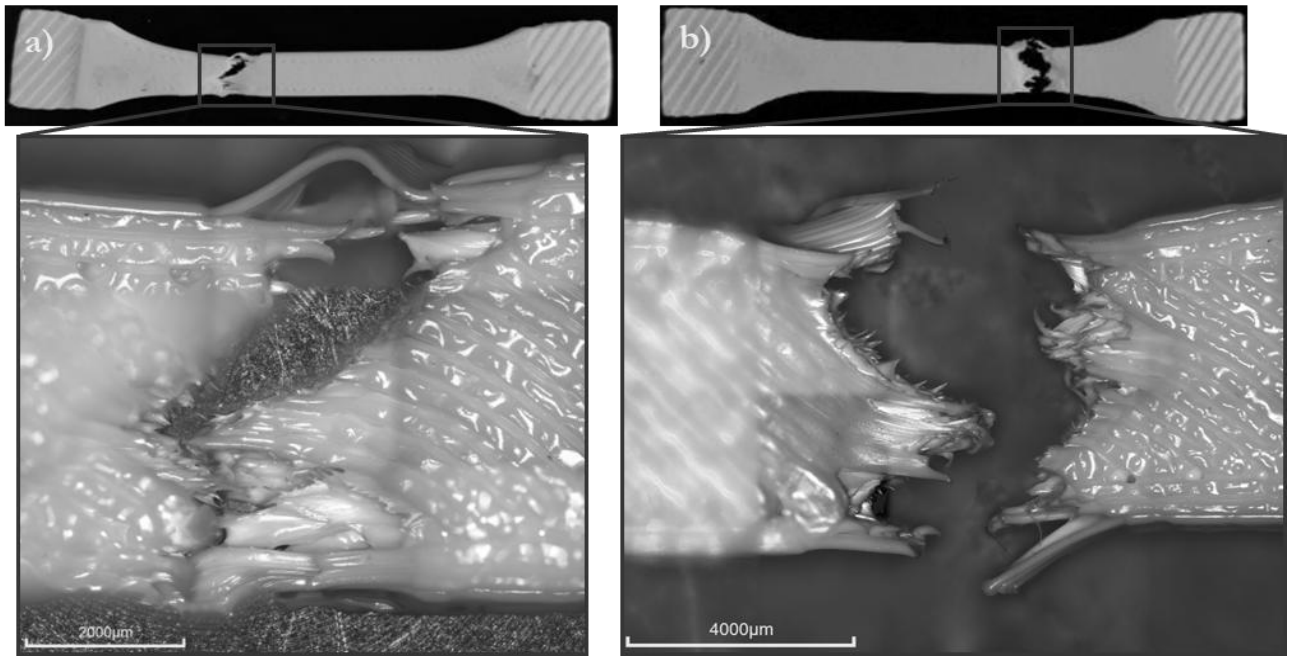

Fig. 6 *Fracture surfaces of PETG samples (100 % infill) after tensile testing observed by confocal microscopy: (a) reference sample (PETG Reference); (b) QUV-aged sample (PETG QUV)*

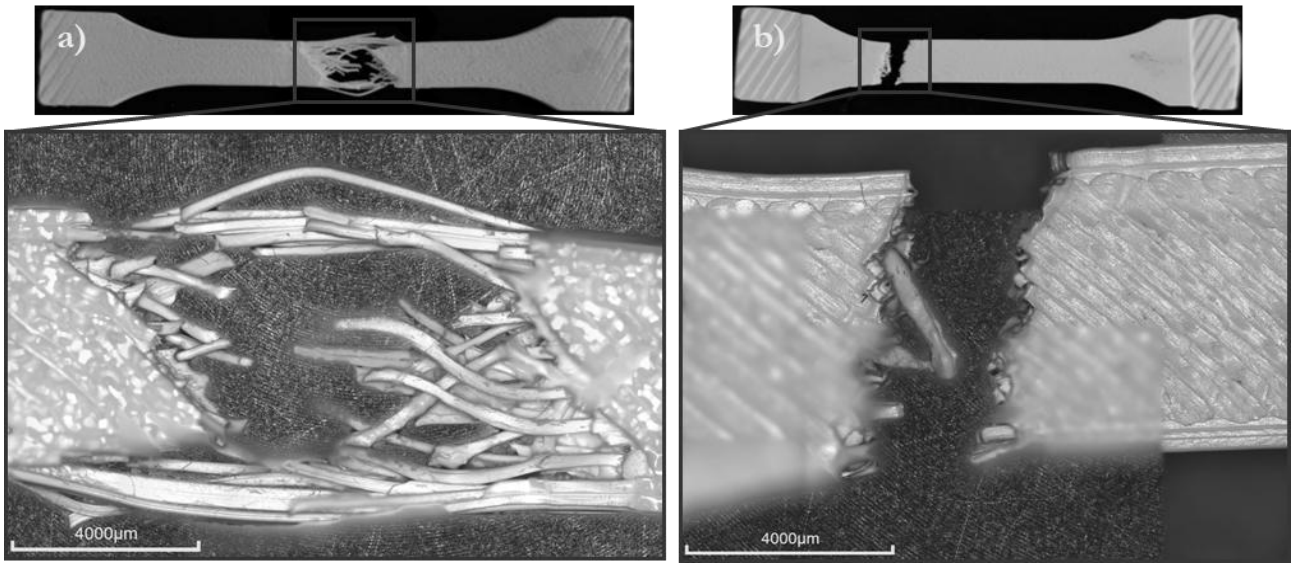

Fig. 7 *Fracture surfaces of PLA samples (100 % infill) after tensile testing observed by confocal microscopy: (a) reference sample (PLA Reference); (b) QUV-aged sample (PLA QUV)*

As presented in Fig. 8, the storage modulus (E') of all analyzed polymers gradually decreased with increasing temperature, indicating the transition from the glassy to the rubbery region. Among the tested materials, PLA exhibited the highest stiffness in the glassy state, reaching approximately 3200 MPa for the reference sample, followed by PETG (~2000 MPa) and ASA (~1900 MPa). These differences correspond to the intrinsic morphology of the polymers, PLA being semi-crystalline, while PETG and ASA possess predominantly amorphous structures with higher chain flexibility [20].

After QUV exposure, ASA showed a noticeable increase in E' in the glassy region, while the post-transition behavior (above T_g) remained nearly identical to the reference, indicating improved stiffness without affecting the viscoelastic relaxation region. PETG also exhibited a slight increase in E', accompanied by a minor upward shift in T_g, suggesting mild structural ordering and improved intermolecular cohesion after aging. In the case of PLA, both the storage modulus increased from approximately 3200 MPa to 3400 MPa and the T_g shifted to a higher temperature, confirming enhanced stiffness and reduced chain mobility as a consequence of secondary crystallization and physical aging [16].

As shown in Fig. 9, the loss modulus (E'') curves of the examined polymers display distinct peaks corresponding to the glass transition temperature (T_g) of each material. The maximum E'' values were recorded for PLA around 65–70 °C, for PETG near 80–85 °C, and for ASA at approximately 115–120 °C. The position and intensity of these peaks represent the molecular mobility of polymer chains during the glass transition [21].

After QUV exposure, noticeable differences were observed mainly for PLA, where the peak intensity of E'' decreased and the T_g slightly increased, indicating reduced chain mobility and increased stiffness as a consequence of secondary crystallization and physical aging. In the case of PETG, the intensity of the loss modulus peak remained almost unchanged, while the T_g shifted slightly to higher temperatures, suggesting a minor increase in structural ordering without significant degradation effects. For ASA, both the peak position and intensity remained nearly identical before and after aging, confirming its excellent stability under UV and humidity exposure.

As shown in Fig. 10, the *tan δ* curves of the tested polymers clearly illustrate the glass transition behavior (T_g) and energy dissipation capacity of each material. The highest damping response was recorded for ASA, reaching a maximum *tan δ* value of approximately 2.4 at around 120 °C. PETG exhibited a peak of about 1.7 slightly below 90 °C, while PLA showed a pronounced peak of 2.1–2.2 near 70 °C in the reference state. These differences reflect the varying degree of chain mobility and amorphous phase content typical for each polymer system [22].

After QUV exposure, the *tan δ* response changed notably for PLA, where the peak intensity decreased sharply to 0.3–0.4 and the T_g shifted to a higher temperature (~75 °C). This behavior indicates restricted molecular motion and increased rigidity due to secondary crystallization and physical aging during accelerated weathering. For PETG, only a minor upward shift in T_g was observed, while the intensity of the peak remained nearly constant, suggesting a slight increase in structural ordering without significant degradation. In the case of ASA, both the position and intensity of the *tan δ* peak remained nearly unchanged, confirming its excellent resistance to UV-induced molecular relaxation processes.

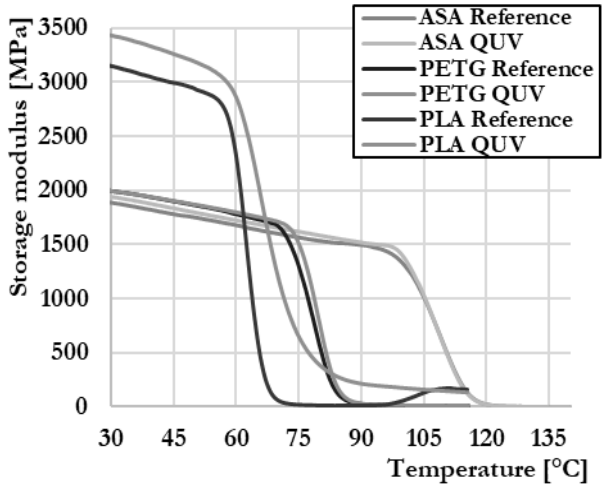

Fig. 8 *Temperature dependence of the storage modulus (E') for ASA, PETG, and PLA materials in reference and QUV-aged states*

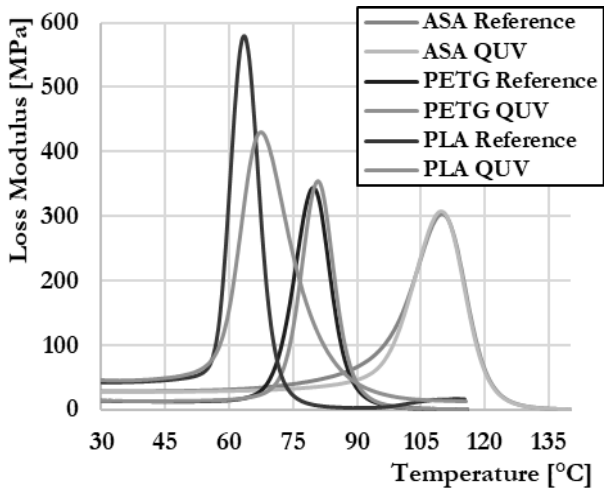

Fig. 9 *Temperature dependence of the loss modulus (E") for ASA, PETG, and PLA materials in reference and QUV-aged states*

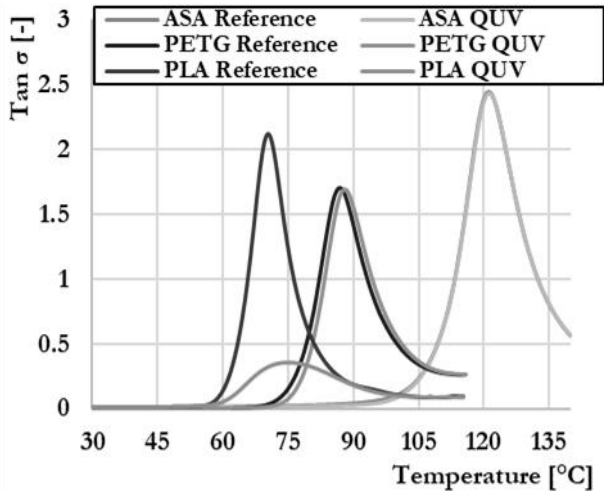

Fig. 10 *Temperature dependence of the tan δ for ASA, PETG, and PLA materials in reference and QUV-aged states*

As shown in Fig. 11, the glass transition temperatures (T_g) of the ASA samples, determined from the peaks of the storage modulus, loss modulus, and loss factor (*tan δ*), remained almost unchanged after QUV exposure. The T_g values derived from the respective curves were approximately 101 °C (storage modulus), 110 °C (loss modulus), and 121 °C (*tan δ*) for the reference sample, compared with 100.9 °C, 109.7 °C, and 121.0 °C for the QUV-aged sample. The minimal variation of less than 0.3% confirms that ASA maintained exceptional thermal and viscoelastic stability under the applied accelerated weathering conditions. The stability of T_g across all evaluation methods indicates that UV radiation and humidity did not induce significant chain scission or molecular relaxation, which correlates well with the unchanged *E'* and *tan δ* behavior observed in the DMA results.

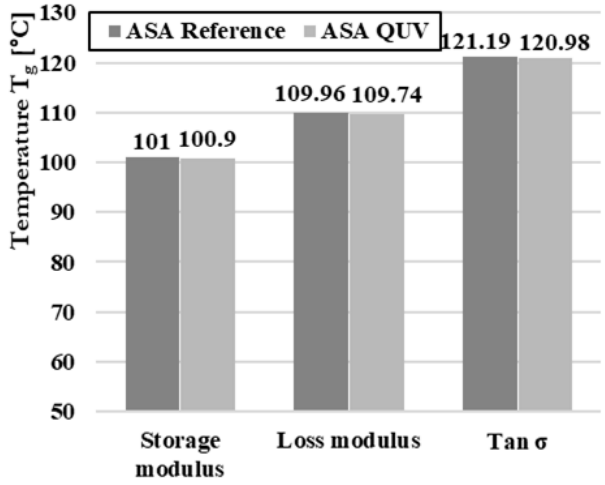

Fig. 11 *Glass transition temperature (T_g) of ASA determined from storage modulus, loss modulus, and tan δ for reference and QUV-aged samples*

As shown in Fig. 12, the glass transition temperatures (T_g) of PETG determined from the storage modulus, loss modulus, and loss factor (*tan δ*) exhibited a slight upward shift after QUV exposure. The T_g derived from the storage modulus increased from 72.41 °C to 74.62 °C, from the loss modulus from 79.52 °C to 80.80 °C, and from *tan δ* from 87.01 °C to 87.82 °C.

This consistent, though minor, increase in T_g across all evaluation methods suggests reduced molecular mobility and mild structural ordering in the amorphous phase of PETG after accelerated weathering. The results indicate that the exposure to UV radiation and humidity did not cause degradation or chain scission, but rather induced slight densification and relaxation of polymer chains, improving thermal stability [23]. The observed behavior aligns with the small increase in *E'* and the negligible change in *tan δ* intensity reported in the DMA curves.

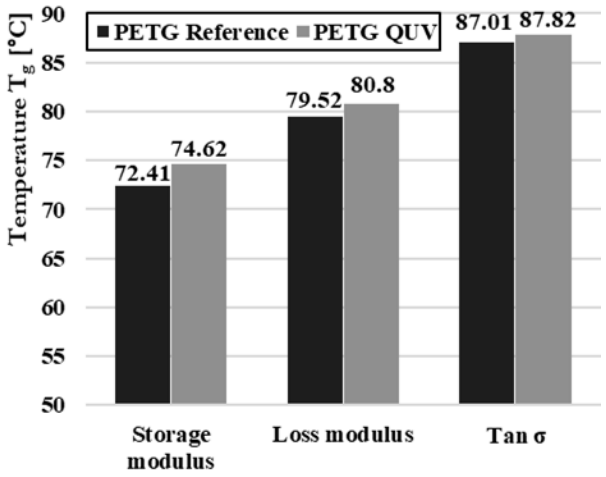

Fig. 12 *Glass transition temperature (T_g) of PETG determined from storage modulus, loss modulus, and tan δ for reference and QUV-aged samples*

As shown in Fig. 13, the glass transition temperatures (T_g) of PLA, determined from the storage modulus, loss modulus, and loss factor (*tan δ*), increased noticeably after QUV exposure. The T_g obtained from the storage modulus rose from 58.71 °C to 59.76 °C, from the loss modulus from 63.49 °C to 67.45 °C, and from *tan δ* from 70.29 °C to 74.93 °C.

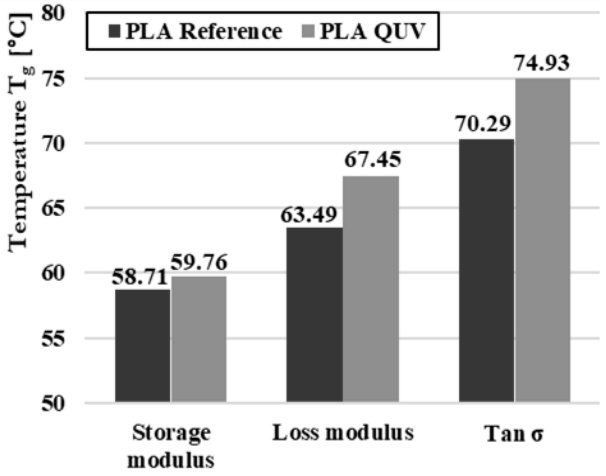

Fig. 13 *Glass transition temperature (T_g) of PLA determined from storage modulus, loss modulus, and tan δ for reference and QUV-aged samples*

This consistent upward shift in T_g across all evaluation methods indicates a reduction in chain mobility and increased structural rigidity caused by secondary crystallization and physical aging during accelerated weathering. The increase in *Tg* corresponds with the higher storage modulus values and the significant decrease in *tan δ* intensity, confirming enhanced stiffness and reduced damping capacity of PLA after exposure. These results suggest that QUV aging promoted molecular ordering rather than degradation, leading to improved thermal and viscoelastic stability of the PLA structure.

The obtained results confirmed that the influence of accelerated weathering on the mechanical and viscoelastic properties of FFF-manufactured polymers is strongly related to their morphological structure. A comparison of ASA, PETG, and PLA revealed distinct differences in their response to UV radiation and humidity cycles, which is consistent with the observations reported by several authors.

For the ASA material, an increase in tensile strength of up to 36% was recorded while maintaining elongation at break between 3.3% and 3.5%. This demonstrates high resistance to photo-oxidation and the stability of the amorphous morphology. Similarly, Sedlák et al. [4] found that no significant loss of ductility occurred after UV and humidity exposure, while Amza et al. [15] reported only minimal changes in modulus and no surface degradation. The fracture analysis performed in this study also confirmed improved interlayer adhesion after aging, which corresponds with the findings of Afshar et al. [18], who pointed out that short-term UV exposure can enhance filament cohesion through molecular chain reorientation.

For PETG, a moderate reduction in tensile strength (≈ 12%) was observed with almost unchanged elongation (4.5–5.3%), suggesting that UV and humidity primarily affected interlayer bonding rather than intrinsic ductility. Similar behavior was reported by Amza et al. [15] and Yost et al. [19], who observed that during physical aging, PETG undergoes mild chain densification and reduced mobility in amorphous regions without severe matrix degradation. The fracture micrographs obtained in this study revealed a transition from smooth, plastically stretched filaments to a rougher, more porous surface with separated filament edges, which is typical for partially brittle behavior resulting from photo-oxidative chain scission.

The PLA samples exhibited the most pronounced change after QUV exposure—the tensile strength increased from 47.6 MPa to 71.9 MPa, accompanied by a slight rise in elongation. This improvement can be attributed to secondary crystallization and physical aging, leading to enhanced stiffness and reduced segmental mobility. Czechowski et al. [16] and Jirků et al. [17] demonstrated that short-term UV irradiation may induce partial molecular ordering in PLA without significant degradation, which corresponds with the observed increase in T_g (from 58.7 °C to 74.9 °C) and storage modulus E' (from 3200 MPa to 3400 MPa). The increase in E' and the upward shift of T_g confirm reduced molecular mobility and improved structural stability of the polymer during accelerated aging.

The comparison of DMA results revealed that all polymers showed a gradual decrease of E' with increasing temperature. However, after QUV testing, an increase in E' in the glassy region and a slight

upward shift in T_g were observed (ASA ≈ +0.3 °C, PETG ≈ +2 °C, PLA ≈ +6 °C). These changes can be interpreted as the result of amorphous phase reorganization and decreased macromolecular mobility caused by secondary crystallization and physical aging.

Overall, the results indicate that short-term exposure to UV radiation and humidity (≈ 80–100 h) can act as a conditioning process that enhances the stiffness and thermal stability of semi-crystalline polymers such as PLA, while amorphous copolymers like PETG remain relatively stable with minimal property variations. ASA proved to be the most stable material for long-term outdoor applications, whereas PLA exhibited the highest potential for short-term strength improvement due to molecular chain reorganization.

4 Conclusion

The study demonstrated that the influence of accelerated weathering on the mechanical and viscoelastic properties of FFF-printed polymers is strongly dependent on their morphological and structural characteristics. Distinct differences were observed among ASA, PETG, and PLA, reflecting the varying sensitivity of amorphous and semi-crystalline polymers to UV radiation and moisture exposure.

ASA exhibited a significant increase in tensile strength (up to 36%) while maintaining elongation at break between 3.3–3.5%. This confirms the excellent environmental stability of ASA and its resistance to UV-induced oxidation. The smoother and more compact fracture surfaces after aging indicate enhanced interlayer adhesion and structural integrity, supporting its suitability for outdoor applications.

PETG showed a moderate decrease in tensile strength (≈ 12%) with almost unchanged ductility (4.5–5.3%). Despite minor photo-oxidative degradation, PETG preserved its plastic deformation capability and maintained good viscoelastic stability.

PLA displayed the most pronounced change in mechanical performance, with a tensile strength increase from 47.6 MPa to 71.9 MPa and a slight rise in elongation. The concurrent increase in storage modulus (E') and T_g confirmed enhanced stiffness and reduced chain mobility due to secondary crystallization and physical aging induced by short-term UV exposure.

The DMA analysis revealed that all polymers experienced a rise in E' in the glassy region and a slight upward shift in T_g after QUV aging, indicating restricted molecular mobility and improved structural ordering. Among the studied materials, ASA maintained the highest long-term stability, PETG exhibited moderate structural resilience, and PLA responded to UV exposure with short-term reinforcement through crystallization.

In summary, the results indicate that moderate QUV exposure (≈ 80–100 h) can act as a conditioning process for selected FFF-printed polymers. While prolonged environmental degradation typically reduces performance, short-term aging may enhance stiffness, cohesion, and viscoelastic stability—particularly in semi-crystalline materials such as PLA and ASA. These findings contribute to the understanding of polymer durability in additive manufacturing and provide guidance for material selection in applications exposed to outdoor environments.

Acknowledgement

This research was supported by the Visegrad Fund Fellowship Program, project ID #62510024. The authors gratefully acknowledge the support provided.

References

[1] PERNICA, J., VODÁK, M., ŠAROCKÝ, R., ŠUSTR, M., DOSTÁL, P., ČERNÝ, M., DOBROCKÝ, D. (2022). Mechanical Properties of Recycled Polymer Materials in Additive Manufacturing. In: *Manufacturing Technology*, Vol. 22, No. 2, pp. 200–203. DOI: 10.21062/mft.2022.017.

[2] ALEXOPOULOU, V. E., CHRISTODOULOU, I. T., MARKOPOULOS, A. P. (2024). Investigation of Printing Speed Impact on the Printing Accuracy of Fused Filament Fabrication (FFF) ABS Artefacts. In: *Manufacturing Technology*, Vol. 24, No. 3, pp. 333–337. DOI: 10.21062/mft.2024.042.

[3] JOSKA, Z., ANDRÉS, L., DRAŽAN, T., MAŇAS, K., POKORNÝ, Z., SEDLÁK, J. (2021). Influence of the Shape of the Filling on the Mechanical Properties of Samples Made by 3D Printing. In: *Manufacturing Technology*, Vol. 21, No. 2, pp. 200–206. DOI: 10.21062/mft.2021.024.

[4] SEDLÁK, J., JOŠKA, Z., JANSKÝ, J., ZOUHAR, J., KOLOMY, Š., SLANÝ, M., SVÁSTA, A., JIROUŠEK, J. (2023). Analysis of the Mechanical Properties of 3D-Printed Plastic Samples Subjected to Selected Degradation Effects. In: *Materials*, Vol. 16, No. 8, pp. 3268. DOI: 10.3390/ma16083268.

[5] ANISKEVICH, A., BULDERBERGA, O., STANKEVICS, L. (2023). Moisture Sorption and Degradation of Polymer Filaments Used in 3D Printing. In: *Polymers*, Vol. 15, pp. 2600. DOI: 10.3390/polym15122600.

[6] BANJO, A. D., AGRAWAL, V., AUAD, M. L., CELESTINE, A. D. N. (2022). Moisture-

Induced Changes in the Mechanical Behavior of 3D Printed Polymers. In: *Composites Part C: Open Access*, Vol. 7, pp. 100243.

[7] AFSHAR, A., WOOD, R. (2020). Development of Weather-Resistant 3D Printed Structures by Multi-Material Additive Manufacturing. In: *Journal of Composites Science*, Vol. 4, No. 3, pp. 94. DOI: 10.3390/jcs4030094.

[8] AMZA, C. G., ZAPCIU, A., BACIU, F., VASILE, M. I., POPESCU, D. (2021). Aging of 3D Printed Polymers under Sterilizing UV-C Radiation. In: *Polymers*, Vol. 13, pp. 4467. DOI: 10.3390/polym13244467.

[9] JUBINVILLE, D., MEKONNEN, T. H. (2025). Enhanced Performance 3-D Printed PLA Parts through a Photo-Initiator-Mediated UV-Curing. In: *Advanced Materials Technologies*, Vol. 10, No. 14, pp. 2500124. DOI: 10.1002/admt.202500124.

[10] ISO 527-2:2012. Plastics — Determination of tensile properties — Part 2: Test conditions for moulding and extrusion plastics. *International Organization for Standardization*, Geneva, Switzerland.

[11] ISO 4892-3:2016. Plastics — Methods of exposure to laboratory light sources — Part 3: Fluorescent UV lamps. *International Organization for Standardization*, Geneva, Switzerland.

[12] KOHUTIAR, M., KRBATA, M., JANÍK, R., FEKIAČ, J. J., KAKOŠOVÁ, L., ESCHEROVÁ, J. (2025). Effect of DCSBD Plasma Treatment on the Mechanical Properties of Polymer Films. In: *Manufacturing Technology*, Vol. 25, pp. 37–44.

[13] ASTM D4065. (2020). Standard Practice for Determining and Reporting Dynamic Mechanical Properties of Plastics. *American Society for Testing Materials*, West Conshohocken, PA, USA.

[14] KUMAR, S. R., SRIDHAR, S., VENKATRAMAN, R., VENKATESAN, M. (2021). Polymer Additive Manufacturing of ASA Structure: Influence of Printing Parameters on Mechanical Properties. In: *Materials Today: Proceedings*, Vol. 39, No. 4, pp. 1316–1319. DOI: 10.1016/j.matpr.2020.04.500.

[15] AMZA, C. G., ZAPCIU, A., PETRESCU, H., POPESCU, D., BACIU, F. (2021). Accelerated Aging Effect on Mechanical Properties of Common 3D Printing Polymers. In: *Polymers*, Vol. 13, No. 23, pp. 4132. DOI: 10.3390/polym13234132.

[16] CZECHOWSKI, L., KEDZIORA, S., MUSEYIBOV, E., SCHLIENZ, M., SZATKOWSKI, P., SZATKOWSKA, M., GRALEWSKI, J. (2022). Influence of UV Ageing on Properties of Printed PLA Containing Graphene Nanopowder. In: *Materials*, Vol. 15, pp. 8135. DOI: 10.3390/ma15228135.

[17] JIRKŮ, P., MULLER, M., MISHRA, R. K., SVOBODOVÁ, J. (2025). Effect of Recycling and UV Ageing on the Properties of PLA-Based Materials Used in Additive Manufacturing. In: *Polymers*, Vol. 17, pp. 1862. DOI: 10.3390/polym17131862.

[18] AFSHAR, A., AL-OBAIDI, M., KHOSRAVANI, M. R. (2020). Development of Weather-Resistant 3D Printed Structures by Multi-Material Additive Manufacturing. In: *Journal of Composites Science*, Vol. 4, No. 3, pp. 94. DOI: 10.3390/jcs4030094.

[19] YOST, S. F., SMITH, J. C., PESTER, C. W., VOGT, B. D. (2025). Physical Aging and Evolution of Mechanical Properties of Additively Manufactured Polyethylene Terephthalate Glycol. In: *RSC Applied Polymers*, Vol. 3, No. 4, pp. 934–947. DOI: 10.1039/D5LP00045A.

[20] KOHUTIAR, M., STUDENÝ, Z., KRBATA, M., JUS, M., MIKUŠ, P., KOVAŘÍKOVÁ, I. (2025). Frequency Dependence of Glass Transition Temperature of Thermoplastics in DMA Analysis. In: *Manufacturing Technology*, Vol. 25, No. 3, pp. 341–347. DOI: 10.21062/mft.2025.043.

[21] KOHUTIAR, M., JANÍK, R., KRBATA, M., FEKIAČ, J. J., KAKOŠOVÁ, L., MIKUŠ, P. (2025). Dynamic Mechanical Analysis of PLA Produced by FFF Additive Manufacturing Technology after DCSBD Plasma Treatment. In: *Manufacturing Technology*, Vol. 25, No. 2, pp. 202–208. DOI: 10.21062/mft.2025.019.

[22] KOHUTIAR, M., PAJTÁŠOVÁ, M., JANÍK, R., PAPUČOVÁ, I., PAGÁČOVÁ, J., PECUŠOVÁ, B., LABAJ, I. (2018). Study of Selected Thermoplastics Using Dynamic Mechanical Analysis. In: *MATEC Web of Conferences*, Vol. 157, pp. 07002. DOI: 10.1051/matecconf/201815707002.

[23] KOHUTIAR, M., JANÍK, R., KRBATA, M., BARTOSOVA, L., JUS, M., TIMÁROVÁ, Ľ. (2023). Study of the Effect of Pretreatment of 3D Printed PLA Filament Modified by Plasma Discharge and Changes in Its Dynamic-Mechanical Properties. In: *Manufacturing Technology*, Vol. 23, No. 4, pp. 461–467. DOI: 10.21062/mft.2023.050.